Paper accepted for presentation at 2009 IEEE Bucharest Power Tech Conference, June 28th - July 2nd, Bucharest, Romania

Optimal Input and Output Signal Selection for Wide-area Controllers

A. M. Almutairi, *Student Member, IEEE* and J. V. Milanović, *Senior Member, IEEE*

***Abstract*—The paper proposes a new method of optimal input and output signal selection for wide-area controllers. The selection procedure employs the Sequential Orthogonalization (SO) algorithm. The method uses the geometric measures of controllability and observability. The selection method is illustrated on the New England Test System (NETS). Results showed applicability of the method for wide-area damping control applications.**

***Index Terms*—controllability, input/output signal selection, geometric measures, observability, Phasor Measurement Unit (PMU), PMU placement, wide-area control.**

I. Introduction

The Sequential Orthogonalization (SO) algorithm has been proposed in [1] for the optimal placement of angle transducers where complete observability of the system interarea modes is targeted. The algorithm places angle transducers, which equivalently can be considered as the phasor measurement units (PMUs), at locations which have the maximum, uncorrelated and non-redundant, observability of the interarea modes and at the same time with the least sensitivity to the local modes. The algorithm applies the *Gram Schmidt* orthogonalization procedure [2] to the rows of the mode observability matrix [3]. The orthogonalization process is aimed to make the selection for only those measurement locations which have the least uncorrelated observability of the interarea modes. Therefore, the number of selected sites for angle transducer installations will be minimized and the redundancy of information (measurements) will be reduced as well. The main feature of the SO algorithm is that it places PMUs at locations situated geographically, and coherently, far away from each other.

It has been shown in [4] that when using remote input/output control signals in a wide-area control system (WACS) the damping of the interarea modes can be highly improved. The wide-area controller processes the system output signals, inputs to the controller, and produces the control signals, outputs of the controller, as added inputs at each generator's exciter reference voltage summation point. The main issue here is to decide from which generators the output signals should be selected and to which generators should the controller signals be sent. In order to increase the effectiveness of the wide-area controller the selected set of input and output signals should have the maximum controllability and observability, respectively, among all possible sets. In addition the number of input and output signals should be minimized to reduce the controller's complexity and the associated communication costs.

The optimal placement problem of PMUs with the aim of maximum observability of interarea modes can be considered equivalent to the problem of the system output (input to the wide-area controller) control signal selection in a wide-area control system. Both of the two problems have the objective of obtaining the maximum observability of the interarea modes using the minimum number of PMUs or output signals. Therefore, the selected optimal PMU locations using the SO algorithm will be considered as the optimal output signals of the system to be feeded-back as inputs to the wide-area controller.

The SO algorithm was applied in [1] for the selection of output measurement locations only, i.e. angle transducers. In fact, the selection methodology based on system observability can be applied equivalently to handle the system controllability; where the system mode controllability matrix is used instead. In this way the system input signals (controller's outputs) can be optimally selected using the SO algorithm.

The mode observability matrix used in the SO algorithm is constructed using the residue-based observability factors [5] for each output in the system. The mode observability matrix however can be constructed using the geometric measures of observability [6]. The geometric measures of observability are dimensionless as they are derived from the cosine of the angle between the output vector and right eigenvector. The residue-based observability factors on the other side suffer a scaling problem when different output types are involved [7]. In addition, it has been shown in [8] that the selections of input and output signals based on the geometric measures of controllability and observability are more robust and more reliable. Therefore the geometric measures of controllability and observability will be used in this study to select the optimal input and output signals, respectively.

In this paper input and output signals are optimally selected for wide-area controllers. The selection procedure applied is based on the SO algorithm where the geometric measures of controllability and observability are used. The objective is to obtain the maximum controllability and observability of the system electromechanical modes of interest, e.g. interarea or least damped modes, while having at the same time the least sensitivity to other modes, e.g. local or highly damped modes.

The authors are with the School of Electrical and Electronic Engineering, The University of Manchester, PO Box 88, Manchester, M60 1QD, UK. (e-mail: a.almutairi@postgrad.manchester.ac.uk, milanovic@manchester.ac.uk).

978-1-4244-2235-7/09/$25.00 ©2009 IEEE

The number of selected input and output signals is also minimized. In addition, the locations of selected signals are also specified.

The selection method is applied to the New England test system. Results of the method are used to design a wide-area controller. The effectiveness of the method is illustrated using small and large disturbance analysis.

II. Selection of Input and Output Signals

A. Measures of Controllability and Observability

Consider the state space representation of a linearized power system [3]

$$\Delta\dot{\boldsymbol{x}}(\boldsymbol{t}) = \boldsymbol{A}\Delta\boldsymbol{x}(\boldsymbol{t}) + \boldsymbol{B}\Delta\boldsymbol{u}(\boldsymbol{t}) \quad (1)$$

$$\Delta\boldsymbol{y}(\boldsymbol{t}) = \boldsymbol{C}\Delta\boldsymbol{x}(\boldsymbol{t}) \quad (2)$$

The system can be transformed to the modal representation as follows

$$\begin{aligned}\dot{\boldsymbol{z}}(\boldsymbol{t}) &= \boldsymbol{F}\boldsymbol{z}(\boldsymbol{t}) + \boldsymbol{G}\Delta\boldsymbol{u}(\boldsymbol{t}) \\ &= \left(\Phi^{-1}\boldsymbol{A}\Phi\right)\boldsymbol{z}(\boldsymbol{t}) + \left(\Psi^{T}\boldsymbol{B}\right)\Delta\boldsymbol{u}(\boldsymbol{t})\end{aligned} \quad (3)$$

$$\begin{aligned}\boldsymbol{y}(\boldsymbol{t}) &= \boldsymbol{H}\boldsymbol{z}(\boldsymbol{t}) \\ &= \left(\boldsymbol{C}\Phi\right)\boldsymbol{z}(\boldsymbol{t})\end{aligned} \quad (4)$$

where $\boldsymbol{F}$ is a diagonal matrix containing the eigenvalues of the $\boldsymbol{A}$ matrix on its diagonal, $\boldsymbol{G}$ is the mode controllability matrix, $\boldsymbol{H}$ is the mode observability matrix, $\boldsymbol{\Phi}$ is matrix of left eigenvectors, and $\boldsymbol{\Psi}$ is matrix of right eigenvectors. Each entry of the $\boldsymbol{G}$ and $\boldsymbol{H}$ matrices is computed, respectively, as follows

$$\boldsymbol{f}_{ci}(\boldsymbol{k}) = \boldsymbol{b}_i^{T}\boldsymbol{\psi}_k \quad (5)$$

$$\boldsymbol{f}_{oj}(\boldsymbol{k}) = \boldsymbol{c}_j\boldsymbol{\phi}_k \quad (6)$$

where $\boldsymbol{f}_{ci}(\boldsymbol{k})$ is the kth modal controllability factor for the ith input and $\boldsymbol{f}_{oj}(\boldsymbol{k})$ in the kth modal observability factor for the jth output.

The $\boldsymbol{G}$ and $\boldsymbol{H}$ matrices are constructed in (3) and (4) using the residue-based modal controllability/observability factors of (5) and (6), respectively. A dimensionless alternative of the mode controllability/observability matrices, to be called $\boldsymbol{G}_m$ and $\boldsymbol{H}_m$, is by using the geometric measures of controllability/observability. The geometric measures of controllability and observability are computed as follows [6]

$$\boldsymbol{m}_{ci}(\boldsymbol{k}) = \cos\left(\alpha\left(\boldsymbol{\psi}_k, \boldsymbol{b}_i\right)\right) = \frac{\left|\boldsymbol{b}_i^{T}\boldsymbol{\psi}_k\right|}{\left\|\boldsymbol{\psi}_k\right\|\left\|\boldsymbol{b}_i\right\|} \quad (7)$$

$$\boldsymbol{m}_{oi}(\boldsymbol{k}) = \cos\left(\theta\left(\boldsymbol{\phi}_k, \boldsymbol{c}_j^{T}\right)\right) = \frac{\left|\boldsymbol{c}_j\boldsymbol{\phi}_k\right|}{\left\|\boldsymbol{c}_j\right\|\left\|\boldsymbol{\phi}_k\right\|} \quad (8)$$

where $|\boldsymbol{z}|$ and $\|\boldsymbol{z}\|$ are the modulus and Euclidean norm of $\boldsymbol{z}$ respectively, $\alpha\left(\boldsymbol{\psi}_k, \boldsymbol{b}_i\right)$ is the geometrical angle between the ith input vector $\boldsymbol{b}_i$ and the kth left eigenvector $\boldsymbol{\psi}_k$, and $\theta\left(\boldsymbol{\phi}_k, \boldsymbol{c}_j^{T}\right)$ is the geometrical angle between the jth output vector $\boldsymbol{c}_j$ and the kth right eigenvector $\boldsymbol{\phi}_k$. The angle between the left eigenvectors and the columns of the input matrix $\boldsymbol{B}$ determines the controllability measure. Similarly the angle between the right eigenvectors and the rows of the output matrix $\boldsymbol{C}$ determines the observability measure. The residue equivalent is the joint controllability and observability measure,

$$\boldsymbol{m}_{cok}(\boldsymbol{i}, \boldsymbol{j}) = \boldsymbol{m}_{ci}(\boldsymbol{k})\boldsymbol{m}_{oj}(\boldsymbol{k}) \quad (9)$$

B. The Sequential Orthogonalization Algorithm

For the selection of the optimal output signals, consider the mode observability matrix $\boldsymbol{H}_m$ constructed using the geometric measures of observability where its rows correspond to p output measurements and its columns corresponding to n system modes. Let the number of the electromechanical modes of interest be n_I and the number of other electromechanical modes be n_L. Form a $p \times n_I$ matrix $\boldsymbol{H}_{mI}$ from the columns of $\boldsymbol{H}_m$ corresponding to the electromechanical modes of interest and a $m \times n_L$ matrix $\boldsymbol{H}_{mL}$ from the columns of $\boldsymbol{H}_m$ corresponding to the other electromechanical modes. The observability of the modes of interest through each output measurement is computed through the norm of the corresponding row of $\boldsymbol{H}_{mI}$. However it is desirable to take the observability of the other modes into consideration. One way of achieving this is by computing a weighting factor as follows [1]

$$\boldsymbol{w}_i = \boldsymbol{\varepsilon} + \frac{\left\|\boldsymbol{h}_{Li}\right\|_2}{\left\|\boldsymbol{h}_{Ii}\right\|_2} \quad (10)$$

where $\boldsymbol{h}_{Li}$ is the ith row of $\boldsymbol{H}_{mL}$ and $\boldsymbol{h}_{Ii}$ is the ith row of $\boldsymbol{H}_{mI}$, $\boldsymbol{\varepsilon}$ is a constant determining the sensitivity to the other modes, and $\|\ \|_2$ is the Euclidean norm of a vector. The higher the value of $\boldsymbol{\varepsilon}$, the higher the toleration of the effects of other modes.

When each row of $\boldsymbol{H}_{mI}$ is divided by the corresponding weighting factor it will yield the weighted modal observability of the corresponding output measurement to the modes of interest. Let the modified rows of $\boldsymbol{H}_{mI}$ be grouped to form the weighted modal observability matrix, $\boldsymbol{Q}$. The values of norms for each row in $\boldsymbol{Q}$, i.e. $\|\mathbf{q}_i\|_2$, will give a measure of the observability of the modes of interest from each output measurement. In addition, it considers the sensitivity to the other modes.

The SO algorithm starts the first selection of output measurement (location) to the one which has the highest weighted modal observability, i.e. the highest $\|\mathbf{q}_i\|_2$. The first selected location will be denoted as the reference location. The subsequent locations are then selected based on the sequential orthogonalization of the corresponding rows of $\boldsymbol{Q}$ to the reference location. The sequential orthogonalization process is performed using the *Gram Schmidt* procedure. Full details of the orthogonalization process can be found in [1].

Each subsequent selection is based on adding sufficient new information, i.e. weighted modal observability, to the set of previous selections. The algorithm stops the selection procedure when there is no new and sufficient information that can be added by the rest of subsequent candidate locations. Therefore the minimum number of output measurements is determined as well as their locations while having the maximum non-redundant observability information on the modes of interest. Therefore the SO algorithm ensures the

non-redundancy of the observability information seen through the selected output measurements (locations).

The selection of the optimal input (control) signals is performed similarly by applying the SO algorithm on the transpose of the mode controllability matrix $\boldsymbol{G_m}$ constructed using the geometric measures of controllability. In $\boldsymbol{G_m}$ columns are corresponding to *m* input (control) signals and rows are corresponding to *n* system modes. The SO algorithm will select a minimum number of input (control) signals, as well as their locations, which have the maximum controllability of the modes of interest among all possible input sets. Similar to the selection of output signals, the SO algorithms ensures the non-redundancy of controllability achieved through the selected input (control) signals.

C. The Wide-area Control Configuration

The wide-area control configuration is illustrated in Fig. 1. The wide-area controller provides a supplementary control signal V_{WAC} through the Automatic Voltage Regulator (AVR) added together with the existing PSS signal V_{PSS}. The wide-area control signals are not sent to all generators in the network but only to a selected sub-set of generators. Similarly, the inputs to the WAC are coming from a selected sub-set of generators.

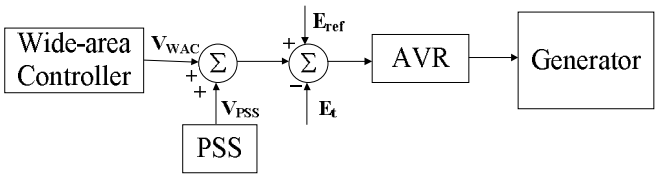

Fig. 1. Wide-area control configuration

The multivariable control configuration of the power system is shown in Fig. 2. Note that input reference signals are omitted in the figure for simplicity. The Multi-Input Multi-Output (MIMO) power system has *m* inputs (candidate outputs of the controller) and *p* outputs (candidate inputs to the controller). A pre-selected set of system outputs [$y_1 \dots y_{p1}$] is fed-back through the control loop to the wide-area controller. Similarly, a pre-selected set of system control inputs [$u_1 \dots u_{m1}$] is sent to the system. Therefore, the MIMO power system will have its outputs reduced from *p* to p_1 and similarly its inputs reduced from *m* to m_1. The reduced set of input and output signals will be obtained by the SO algorithm.

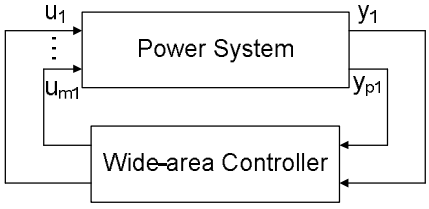

Fig. 2. Input/output signals for multivariable control of power system

III. Case Study

The geometric measure based input and output signal selection method is applied to the meshed 39-bus 10-machine New England Test System (NETS) shown in Fig. 3 [9, 10]. The NETS system was modeled in the Matlab and Simulink environment. Models and data of the AVRs and PSSs are shown in the appendix. The simulated and linearized system has 10 inputs, at E_{ref} of each generator, and 10 output measurements, generator speed. The system eigenvalues corresponding to the electromechanical modes are listed in Table I. Modes 7-9 are considered (arbitrarily for the purpose of illustrating proposed methodology) as the modes of interest. The geometric measures of controllability and observability are computed for the linearized system and are shown in Table II and Table III, respectively.

TABLE I
EIGENVALUES LOCATIONS CORRESPONDING TO THE ELECTROMECHANICAL MODES

Mode	Eigenvalues [1/s +j rad/s]	Damping Ratio	Frequency [Hz]
Mode#1	-2.67 ± j 9.38	27.42	1.49
Mode#2	-1.51 ± j 8.96	16.62	1.43
Mode#3	-1.78 ± j 9.03	19.40	1.44
Mode#4	-2.49 ± j 8.14	29.25	1.30
Mode#5	-0.53 ± j 7.42	7.12	1.18
Mode#6	-1.99 ± j 7.55	25.54	1.20
Mode#7	-1.52 ± j6.89	21.47	1.10
Mode#8	-1.68 ± j6.79	24.08	1.08
Mode#9	-0.44 ± j2.55	17.13	0.41

The matrix of geometric measures of controllability $\boldsymbol{G_m}$ is constructed and the SO algorithm is applied. The optimal selected input signals are listed in Table IV. It can be seen that the input signals are minimized to only 3 locations for generators located far away from each other.

The SO algorithm is then applied by considering the geometric measures of observability, i.e. $\boldsymbol{H_m}$ matrix. The optimal selected output locations are listed in Table IV. As for the selected input signals of the system, it can be seen that the number of those output locations is also minimized to only 3 locations for generators located far away from each other. The selected optimal input and output signal locations are shown in Fig. 3.

IV. Assessment of the Selection Method

A. Application of selected input/output signals to WAC

The selection method was assessed by applying a wide-area controller to the NETS system in the closed-loop, as in Fig. 2. The closed-loop system is formed based on the results of input and output signals selection by the SO algorithm.

The wide-area controller (WAC) is designed based on the Linear Quadratic Gaussian (LQG) control [11]. Inputs of the closed-loop system, i.e. controller outputs, are the

supplementary control signals added at each AVR summation point of generators chosen by the SO algorithm based on controllability. Outputs of the closed-loop system, i.e. controller inputs, are active power, terminal voltage, and speed deviation of generators chosen by the SO algorithm based on observability. The terminal voltage and active power measured signals were added, in addition to speed deviation, to increase the accuracy of the estimation process by the Kalman filter and hence the robustness of the LQG controller.

TABLE II
GEOMETRIC MEASURES OF CONTROLLABILITY

Input Location	G1	G2	G3	G4	G5	G6	G7	G8	G9	G10
Mode#1	0.35	0.12	0.11	0.09	0.06	0.19	0.15	1.00	0.18	0.31
Mode#2	0.35	1.00	0.28	0.05	0.04	0.02	0.24	0.22	0.07	0.17
Mode#3	0.05	0.07	0.03	0.04	0.02	0.63	1.00	0.04	0.02	0.04
Mode#4	0.50	0.18	0.31	0.03	0.06	0.88	1.00	0.97	0.58	0.89
Mode#5	0.08	0.01	0.04	1.00	0.34	0.09	0.14	0.02	0.03	0.05
Mode#6	0.16	0.11	0.40	0.43	1.00	0.26	0.29	0.26	0.49	0.31
Mode#7	0.11	0.04	0.43	0.08	0.09	0.05	0.06	0.06	1.00	0.11
Mode#8	0.25	0.13	1.00	0.10	0.09	0.06	0.08	0.06	0.48	0.11
Mode#9	1.00	0.26	0.45	0.63	0.64	0.57	0.68	0.29	0.53	0.45

TABLE III
GEOMETRIC MEASURES OF OBSERVABILITY

Output Location	G1	G2	G3	G4	G5	G6	G7	G8	G9	G10
Mode#1	0.01	0.17	0.13	0.10	0.15	0.24	0.21	1.00	0.16	0.27
Mode#2	0.01	1.00	0.23	0.05	0.04	0.03	0.13	0.08	0.03	0.10
Mode#3	0.00	0.14	0.05	0.03	0.04	0.80	1.00	0.08	0.03	0.05
Mode#4	0.01	0.21	0.26	0.18	0.55	1.00	0.81	0.80	0.38	0.68
Mode#5	0.00	0.02	0.08	1.00	0.27	0.10	0.13	0.02	0.07	0.04
Mode#6	0.01	0.01	0.05	0.48	1.00	0.19	0.23	0.10	0.11	0.15
Mode#7	0.01	0.04	0.32	0.15	0.27	0.09	0.07	0.15	1.00	0.17
Mode#8	0.02	0.17	1.00	0.15	0.26	0.10	0.10	0.12	0.54	0.13
Mode#9	0.57	0.34	0.43	0.62	1.00	0.85	0.84	0.51	0.59	0.42

TABLE IV
OPTIMAL SELECTED SETS OF INPUT AND OUTPUT SIGNALS

Selection no.	Optimal Inputs to the system (based on controllability)	Optimal Outputs from the system (based on observability)
1st.	G3	G1
2nd.	G6	G3
3rd.	G9	G9

B. Small Disturbance Stability Assessment

The damping ratio for each electromechanical mode is computed for the closed-loop system and is listed in Table V. The table shows also the achieved improvement in the damping ratio. Improvement is computed as the difference between the damping ratio of the mode in the open-loop system (without WAC) and the damping ratio of the same mode in the closed-loop system (with WAC). It can be seen

TABLE V
DAMPING RATIOS OF THE ELECTROMECHANICAL MODES OF THE OPEN-LOOP AND CLOSED LOOP SYSTEMS

Mode	Open-loop System	Closed-loop System	Improvement in Damping Ratio
Mode#1	27.42	27.78	0.37
Mode#2	16.62	16.94	0.32
Mode#3	19.40	19.87	0.47
Mode#4	29.25	30.69	1.43
Mode#5	7.12	7.15	0.02
Mode#6	25.54	25.76	0.22
Mode#7	21.47	57.31	35.84
Mode#8	24.08	30.62	6.55
Mode#9	17.13	20.99	3.86

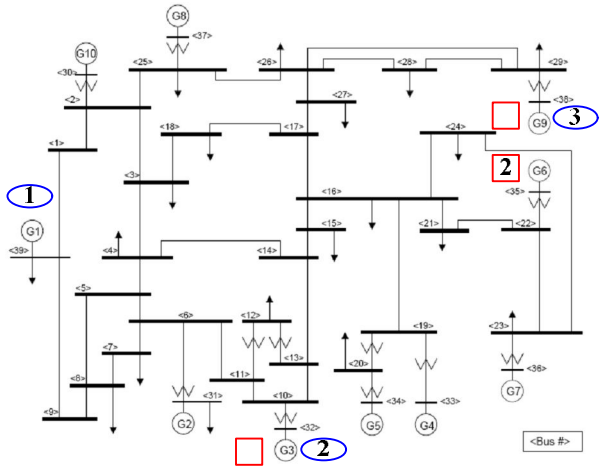

Fig. 3. New England test system [10] with optimal input and output signal locations. Input locations are identified by squares and output locations (measurement points) by ovals. All locations are numbered according to the selection sequence.

from Table V that the damping ratios of the modes of interest, modes 7-9, have been improved significantly in the closed-loop system. It can be seen also that the damping ratios of other modes, i.e. modes 1-6, have not changed largely. This shows the effectiveness of the input and output signal selection using the SO algorithm on the chosen set of modes of interest.

C. Transient Stability Assessment

The large disturbance (transient) stability assessment of the closed-loop system was also performed. A three phase, self-clearing fault lasting 4 cycles, was simulated at bus 16 in the open-loop and the closed-loop systems. The resulting speed responses of generators 1, 3 and 9 are shown in Fig. 4, 5, and 6, respectively. It can be seen from the figures that the wide-area controller designed with reduced number of input and output signals chosen by the SO algorithm effectively enhances the stabilization of the system.

V. Conclusions

A selection method of input and output signals for wide-area controllers is proposed. The method is based on the SO algorithm. The method reduces the number of required input and output signals and specifies their locations. The reduced set of input and output signals provides the maximum controllability and observability for the electromechanical modes of interest. In addition, it provides non-redundant controllability and observability information.

The method was illustrated on the New England test system. Results of the selection method were assessed by applying a wide-area controller. Small disturbance analysis results showed the effectiveness of the method in enhancing the damping ratios of the modes of interest. Large disturbance analysis results also showed that the wide-area controller designed based on the selected input and output signals improves the stability of the power system.

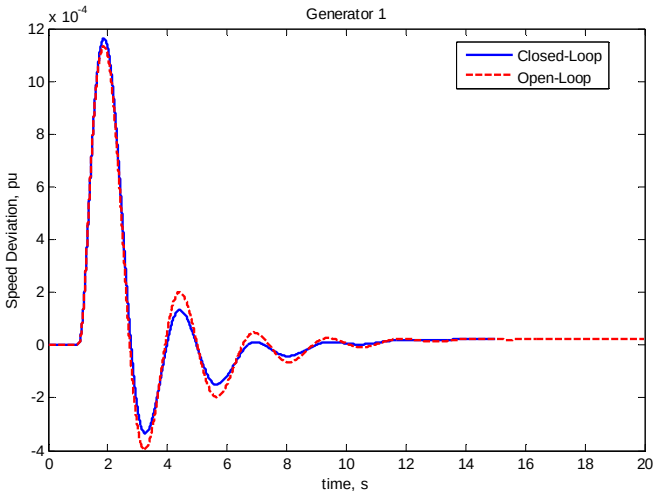

Fig. 4. Speed deviation responses of generator 1 for a three phase fault at bus#16

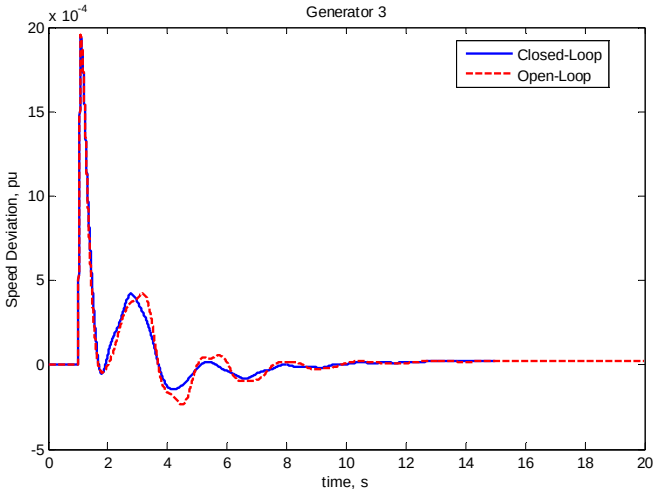

Fig. 5. Speed deviation responses of generator 3 for a three phase fault at bus#16

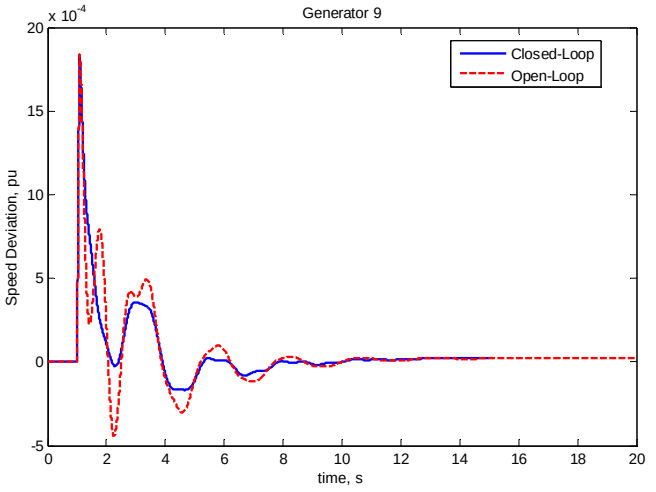

Fig. 6. Speed deviation responses of generator 9 for a three phase fault at bus#16

APPENDIX

TABLE VI
PSS PARAMETERS

Generator	K_{PSS}	T_1	T_2	T_3	T_4
G1	20	0.8685	0.44689	0	0
G2	17	0.4742	0.1179	0.4742	0.1179
G3	8	0.4559	0.13156	0.4559	0.13156
G4	26	0.4247	0.09687	0.4247	1.09687
G5	10	0.5538	0.1291	0.5538	0.1291
G6	9	0.5056	0.1007	0.5056	0.1007
G7	8	0.4264	0.1071	0.4264	0.1071
G8	8	0.4594	0.08113	0.4594	0.08113
G9	10	0.7820	0.0925	0	0
G10	25	0.5339	0.1037	0.5339	0.1037

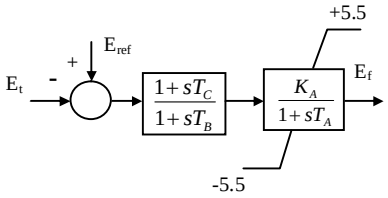

Fig. 7. AVR model (IEEE type AC4A excitation system model)

The parameters of the AVRs are:
T_A=0.055, T_B=10, T_C=2, K_A=198.

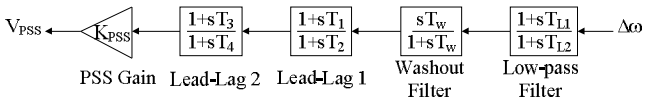

Fig. 8. PSS model

The parameters of the local PSSs are:
T_{L1}=0.0563, T_{L2}=0.1125, T_w=10.

REFERENCES

[1] E. W. Palmer and G. Ledwich, "Optimal placement of angle transducers in power systems," *IEEE Trans. Power Syst.*, vol. 11, pp. 788-793, 1996.
[2] B. Noble and J. W. Daniel, "*Applied Linear Algebra*", Englewood Cliffs: Prentice-Hall Inc., 1988.
[3] P. Kundur, "*Power System Stability and Control*": McGraw Hill, 1993.
[4] M. E. Aboul-Ela, A. A. Sallam, J. D. McCalley, and A. A. Fouad, "Damping controller design for power system oscillations using global signals," *IEEE Trans. Power Syst.*, vol. 11, pp. 767-773, 1996.
[5] N. Martins and L. T. G. Lima, "Determination of suitable locations for power system stabilizers and static VAR compensators for damping electromechanical oscillations in large scale power systems," *IEEE Trans. Power Syst.*, vol. 5, pp. 1455-1469, 1990.
[6] A. M. A. Hamdan and A. M. Elabdalla, "Geometric measures of modal controllability and observability of power system models," *Elect. Power Syst. Research*, vol. 15, pp. 147-155, 1988.
[7] I. Kamwa, R. Grondin, and Y. Hebert, "Wide-area measurement based stabilizing control of large power systems-a decentralized/hierarchical approach," *IEEE Trans. Power Syst.*, vol. 16, pp. 136-153, 2001.
[8] A. Heniche and I. Kamwa, "Assessement of two methods to select wide-area signals for power system damping control," *IEEE Trans. Power Syst.*, vol. 23, pp. 572-581, May 2008.
[9] R. D. Zimmerman, C. E. Murillo-Sánchez, and D. Gan, "MATPOWER", http://www.pserc.cornell.edu/matpower/.
[10] http://psdyn.ece.wisc.edu/IEEE_benchmarks/index.htm.
[11] J. M. Maciejowski, "*Multivariable Feedback Design*", UK: Addison-Wesley, 1989.

Abdulaziz M. Almutairi (S'2006) received the B.Sc. degree from Kuwait University, Kuwait, and the M.Sc. degree form the University of North Carolina at Charlotte, NC, USA, all in Electrical Engineering.

He is currently working towards his Ph.D. in the School of Electrical and Electronic Engineering at The University of Manchester, UK.

Jovica V. Milanović (M'95, SM'98) received his Dipl.Ing. and his M.Sc. degrees from the University of Belgrade, Yugoslavia, his Ph.D. degree from the University of Newcastle, Australia, and his Higher Doctorate (D.Sc. degree) from The University of Manchester, UK, all in Electrical Engineering.

Currently, he is a Professor of electrical power engineering and Deputy Head of School (Research) in the School of Electrical and Electronics Engineering at The University of Manchester, UK.